

# The Perspective of Cooperative Hydrotropy on the Solubility in Aqueous Solutions of Cyrene

Dinis O. Abranches, Jordana Benfca, Seishi Shimizu, and João A. P. Coutinho\*

Cite This: <https://dx.doi.org/10.1021/acs.iecr.0c02346>

Read Online

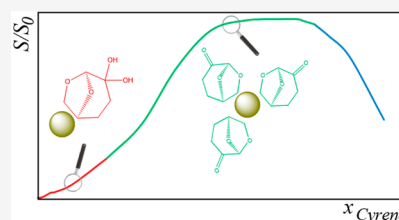
ACCESS |

Metrics & More

Article Recommendations

Supporting Information

**ABSTRACT:** Cyrene is an emerging biobased green solvent that has been shown to have the ability to increase the solubility of hydrophobic substances in water. Even though the water–Cyrene system is an attractive solvent, its applications are hampered by difficulties in the understanding of its solvation mechanism, caused by a delicate chemical equilibrium established between water and Cyrene. This work aims to rationalize the solvent capability of the water–Cyrene system and to establish the mechanisms of solvation through which hydrophobic solutes are dissolved in it. Using the cooperative model of hydrotropy, it is shown that hydrotropy is the solubilization mechanism of hydrophobic solutes in the water–Cyrene system, in most of its concentration range. Furthermore, the ketone form of Cyrene is revealed to be the principal hydrotrope of the system, with the diol form acting as a hydrotrope only at low Cyrene concentration. The parameters of the cooperative model, namely, the number of hydrotrope molecules aggregated around the solute and the maximum solubility increase, are shown to be correlated with the hydrophobicity of the solutes quantified by their octanol–water partition coefficient. This result not only supports recent studies on the mechanism of hydrotropy but also adds a predictive ability to the cooperative model, which is then explored to successfully predict the solubility curves of phthalic acid, aspirin, gallic acid, and vanillin in water–Cyrene mixtures.



## 1. INTRODUCTION

Dihydrolevoglucosenone, more commonly known as Cyrene, is a novel green solvent produced from cellulose in a two-step process.<sup>1–4</sup> A good hydrogen bond accepting capacity, owing to its one carbonyl and two ether groups, makes Cyrene a polar yet aprotic solvent, with properties similar to other aprotic solvents such as *N*-methyl-2-pyrrolidone (NMP). Due to its biodegradability and the abundance of its precursor, Cyrene has attracted considerable interest, with studies showing it to be an excellent medium for a wide variety of chemical reactions,<sup>5–12</sup> including graphene processing.<sup>13</sup>

Recently, Cyrene was reported to be a hydrotrope that could enhance the solubility of various hydrophobic substances.<sup>14</sup> Hydrotropes, when added to water, can greatly increase its capacity to dissolve hydrophobic solutes.<sup>15,16</sup> From a green chemistry perspective, hydrotropy is advantageous in minimizing the need to use organic solvents to process hydrophobic compounds.<sup>17</sup> Moreover, depending on the hydrotropic system composition, addition of water leads to the precipitation of the solute, facilitating its recovery.<sup>18–20</sup> This is particularly interesting with Cyrene since the resulting solvent (water–Cyrene system) is classified as a biobased and biodegradable solvent, whose properties, namely, polarity, can be tuned by changing the concentration of its components.

Despite its appeal, the behavior of solutes in water–Cyrene mixtures is complex due to the reactivity of Cyrene with water. In fact, Cyrene reacts partially and reversibly with water to form the corresponding geminal diol. This geminal diol, in turn, is acidic, partially dissociating in water.<sup>21</sup> In this way,

water–Cyrene mixtures are complex systems containing water, the ketone, and protonated and deprotonated diol forms of Cyrene. Considering that each of these individual species can have a different role (favorable or unfavorable) in the dissolution of a solute, an understanding of this chemical equilibrium is needed to develop the potential of water–Cyrene mixtures for novel applications. De Bruyn et al.<sup>14</sup> pioneered the study of the hydrotropic capacity of water–Cyrene mixtures and concluded that the form of Cyrene responsible for the solubility increase of hydrophobic solutes was the geminal diol form.

Understanding the mechanism of hydrotropy can provide a useful insight as to which component of the water–Cyrene system is responsible for the solubility increase of hydrophobic substances. The cooperative theory of hydrotropy,<sup>22–24</sup> which has recently been supported by experimental evidence,<sup>25</sup> holds that hydrotropy occurs due to the accumulation of hydrotrope molecules around solute molecules. More specifically, water mediates the aggregation of apolar moieties of the hydrotropes around the solute, decreasing the overall apolar surface area contacting water, thus maximizing its hydrogen bonding ability

Received: May 8, 2020

Revised: September 7, 2020

Accepted: September 23, 2020

Published: September 23, 2020

(hydrophobic effect). According to this theory, the major driving force of hydrotropy is the apolarity of both the hydrotrope and the solute, as postulated for the first time by Bauduin et al.<sup>26</sup> Since the ketone and diol forms of Cyrene possess approximately the same apolar surface area, both forms are expected to function as hydrotropes, which is at odds with the original proposal of De bruyn et al.<sup>14</sup> in which the germinal diol was the main component responsible for the hydrotropic behavior of these systems. Such a question is underscored further by a structural point of view: the diol form interacts more extensively with water through hydrogen bonding than the ketone form, meaning that the latter is freer to interact with the solute than the former.

The objective of this work is to provide a theoretical framework on which the solvent capability of the delicate water–Cyrene system can be rationally explored. The data reported by De bruyn et al.<sup>14</sup> for the solubility of salicylic acid, ferulic acid, ibuprofen, and caffeine in the water–Cyrene system, along with novel data for benzoic acid and syringic acid measured in this work, was studied from the perspective of the cooperative hydrotropy model. The correlations obtained between the parameters of this model and the hydrophobicity of the solutes are then explored to predict the solubility curves of phthalic acid and aspirin (data from De bruyn et al.<sup>14</sup>) and of gallic acid and vanillin (data herein measured) in water–Cyrene mixtures.

## 2. EXPERIMENTAL DETAILS

**2.1. Chemicals.** The compounds experimentally used in this work were used as received. Ultrapure water obtained using a Milli-Q plus 185 water purification apparatus (resistivity of 18.2 MΩ·cm at 25 °C and total organic carbon inferior to 5 μg·dm<sup>-3</sup>) was used to perform all solubility experiments. The purity and source details of all compounds used in this work are listed in Table 1. Note that gallic acid monohydrate was experimentally used in the solubility measurements, but the results are reported and analyzed in terms of anhydrous gallic acid.

**Table 1. List of Compounds Experimentally Used in This Work Along With Their CAS Number, Source, and Purity**

compound	CAS number	source	purity (wt %)
Cyrene	53716-82-8	Acros Organics	>99
gallic acid monohydrate	5995-86-8	Merck	>99.5
syringic acid	530-57-4	Acros Organics	>98.0
vanillin	121-33-5	Sigma-Aldrich	>99.0
benzoic acid	65-85-0	Acros Organics	99

**2.2. Solubility Measurements.** The solubility of each solute (gallic acid, syringic acid, vanillin, and benzoic acid) in the water–Cyrene system was measured using what is commonly referred to as the isothermal shake-flask method, previously described in the literature<sup>18,20</sup> and detailed below. The solubility results obtained are reported in Tables S1–S3 of the Supporting Information.

Mixtures of water and Cyrene were prepared to cover the entire composition range of this system, from pure water to pure Cyrene. Excess of solute was added to each mixture and the samples were left to equilibrate under agitation (1050 rpm) at a temperature of either 293.2 ± 0.5 K, for syringic acid and benzoic acid, or 303.2 ± 0.5 K, for gallic acid and vanillin, using Eppendorf Thermomixer Comfort equipment (temper-

ature control uncertainty of 0.5 K). After 72 h, the samples were centrifuged for 20 min in a Hettich Mikro 120 centrifuge at 4500 rpm and a temperature of 293.2 ± 0.5 or 303.2 ± 0.5 K, depending on the solute, to separate the excess solid. Three samples of the liquid phase were carefully collected, diluted in ultrapure water, and their ultraviolet absorbance was measured in a Shimadzu UV-1700, Pharma-Spec spectrometer at a specific wavelength (262 nm for gallic acid, 267 nm for syringic acid, 280 nm for vanillin, and 273 nm for benzoic acid).

**2.3. Cooperative Hydrotropy Model.** Shimizu and Matubayasi<sup>22</sup> developed a statistical thermodynamics-based model (henceforth named cooperative hydrotropy model) to describe hydrotropy. The foundations of this model are presented in Section 1 of this work, namely, that hydrotropy occurs due to water-mediated aggregation of hydrotropes around the solute. The model can be expressed in the following manner

$$\frac{S}{S_0} = \frac{1 + e^{b \left( \frac{S}{S_0} \right)_{\max}} x_H^m}{1 + e^b x_H^m} \quad (1)$$

or in the linearized form

$$\ln \left[ \frac{1 - \frac{S}{S_0}}{\frac{S}{S_0} - \left( \frac{S}{S_0} \right)_{\max}} \right] = m \ln(x_H) + b \quad (2)$$

where  $S$  is the molar solubility (mol/L) of the solute in the hydrotropic system,  $S_0$  is its molar solubility in water (mol/L),  $(S/S_0)_{\max}$  is the maximum attainable relative solubility (the value at the plateau, which a typical hydrotropy solubility curve reaches, henceforth denoted as  $\delta_{\max}$ ), and  $x_H$  is the mole fraction of the hydrotrope (in the hydrotropic system and not on a solute-free basis). Finally,  $m$  and  $b$  are parameters of the model, both with a physical meaning. Parameter  $m$  is the number of hydrotrope molecules involved in the solvation of the solute and parameter  $b$  is related to the facility of inserting that number of hydrotrope molecules in the volume corresponding to the vicinity of the solute.

Although the model can be applied by extracting  $\delta_{\max}$  from the experimental solubility data, this is not always trivial, especially when the solubility curve is not perfectly sigmoidal, as is the case for Cyrene–water mixtures. A way to avoid this problem,<sup>18</sup> which is used in this work, is to leave  $\delta_{\max}$  as the adjustable parameter of the model. Note that parameters  $m$  and  $b$  are obtained by plotting the left-hand side of eq 2 against  $\ln x_H$  and fitting a straight line, meaning that  $\delta_{\max}$  is the sole adjustable parameter of this model.

## 3. RESULTS AND DISCUSSION

**3.1. Cyrene–Water Chemical Equilibria.** Carbonyl functional groups are known to react with water, forming geminal diols. Among other factors, the extent of this chemical equilibrium depends on the stability of the carbonyl group, which in turn depends on the electron-donating ability of its vicinity groups.<sup>27</sup> Ketones are less prone to form geminal diols than aldehydes due to their additional alkyl group, which acts as an electron-donating agent, stabilizing the carbonyl group. The equilibrium constant of acetone and its geminal diol, for example, is 3 orders of magnitude lower than that of acetaldehyde and its geminal diol. Ketones can, nevertheless,

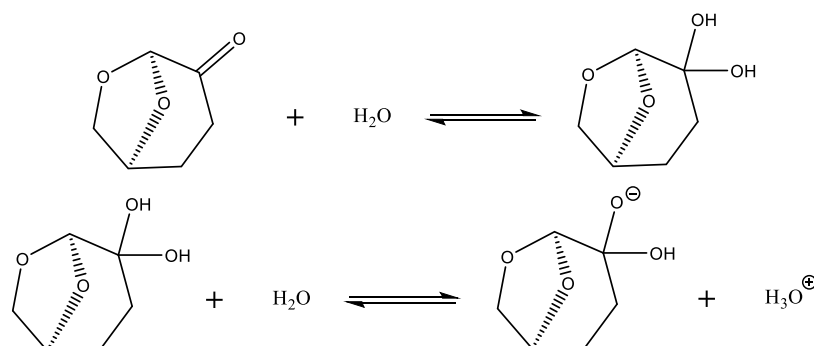


**Figure 1.** Chemical equilibrium of Cyrene and its geminal diol in water (top panel) and dissociation of the geminal diol (bottom panel).

form geminal diols. A typical example is that of hexafluoroacetone, which, due to the electron-withdrawing effect of the fluorine atoms, reveals an equilibrium constant with its diol 9 orders of magnitude higher than that shown by acetone and its diol.<sup>27</sup>

When dissolved in water, Cyrene establishes an equilibrium to form its corresponding geminal diol,<sup>14</sup> as depicted in Figure 1. The extent of this equilibrium is large for a ketone, explained by considering the electron-withdrawing effect of the ether groups in Cyrene, which destabilizes the carbonyl group, in line with the previous paragraph. Moreover, the geminal diol formed partially dissociates, as suggested by the low pH of Cyrene–water mixtures.<sup>21</sup>

De bruyn et al.<sup>14</sup> quantified the concentration of water and the ketone and diol forms of Cyrene present in the water–Cyrene system, over the full concentration range, from pure water to pure Cyrene. They neglected the presence of the dissociated form of the diol (second reaction in Figure 1). As explained in Section S1 of the Supporting Information, this is here justified as a good approximation since the concentration of the dissociated form of the diol is very small, as suggested by the pH of the system. In the absence of a constant equilibrium constant for this system, De bruyn et al.<sup>14</sup> speculated that this parameter changes with the concentration of water, most likely due to strong intermolecular hydrogen bonding between water and the diol form of Cyrene, resulting in large deviations from thermodynamic ideality. The experimental quantification of the various Cyrene forms presented by De bruyn et al.<sup>14</sup> allowed for the calculation of the mole fraction of the ketone and diol forms of Cyrene (both the nondissociated and dissociated geminal diol are considered as the diol form of Cyrene), as explained in Section S2 of the Supporting Information and depicted in Figure 2.

Figure 2 reveals that Cyrene exists in water mostly as its diol form until a mole fraction of about 0.35, where the trend is reversed, and its ketone form becomes predominant. The amount of the geminal diol in the system water–Cyrene is maximum at a mole fraction of total Cyrene of about 0.3. This is important since the maximum in the concentration of the geminal diol should correspond to the maximum in the solubility of a hydrophobic solute, should the geminal diol be the principal form responsible for the hydrotropic ability of Cyrene.

From Figure 1, it may be argued that changing the pH of the system could change the equilibrium of Cyrene in water. This would be problematic when studying acidic solutes, such as those used in this work. However, it is shown in Section S1 of the Supporting Information that setting the pH value of the

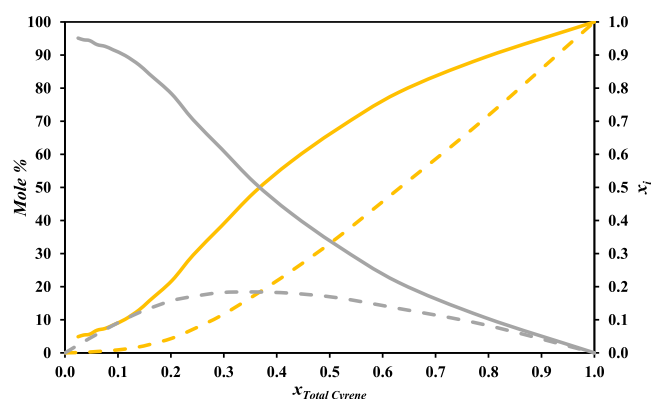


**Figure 2.** Composition of water–Cyrene mixtures: mole percentage (left axis, full lines) and mole fraction (right axis, dashed lines) of the ketone form (yellow full and yellow dashed lines) and the diol form (gray full and gray dashed lines) of Cyrene as a function of its total mole fraction (sum of the mole fractions of the ketone form and the diol form), calculated, as described in the Supporting Information, from the data reported by De bruyn et al.<sup>14</sup> at 298 K.

system to 1 does not significantly impact the water–Cyrene equilibrium.

### 3.2. Hydrotrophy in Aqueous Solutions of Cyrene.

When measuring the solubility of a substance in a multi-component system, it is a common practice to prepare first the solvent with the desired composition and then add the solute. As such, hydrotrophy data is typically reported as the solubility of the solute against the hydrotrope fraction in the solvent (solute-free basis). Even though it is practical, thermodynamic analysis requires this data to be converted to mole fractions in the resulting multicomponent system. This is especially important in the case of Cyrene, since its reaction with water significantly alters the composition of the solvent and that of the final mixture. This conversion is detailed in Section S3 of the Supporting Information. Henceforth, all data is analyzed in terms of the total mole fraction of Cyrene in the final system after equilibrium is achieved ( $x_{\text{total Cyrene}}$ ), defined as the sum of mole fractions of the ketone and diol forms of Cyrene.

To establish the role of each Cyrene species in the solubilization of hydrophobic solutes, solubility data for benzoic and syringic acids, herein experimentally measured, is first discussed. Unlike for other hydrotrope systems, such as those based on glycerol ethers,<sup>18</sup> fitting the cooperative hydrotrophy model to the full concentration range of Cyrene is not possible. Instead, the model needs to be fitted separately to the region of  $x_{\text{total Cyrene}}$  between 0 and about 0.2 and to the region of  $x_{\text{total Cyrene}}$  between about 0.2 and the mole fraction

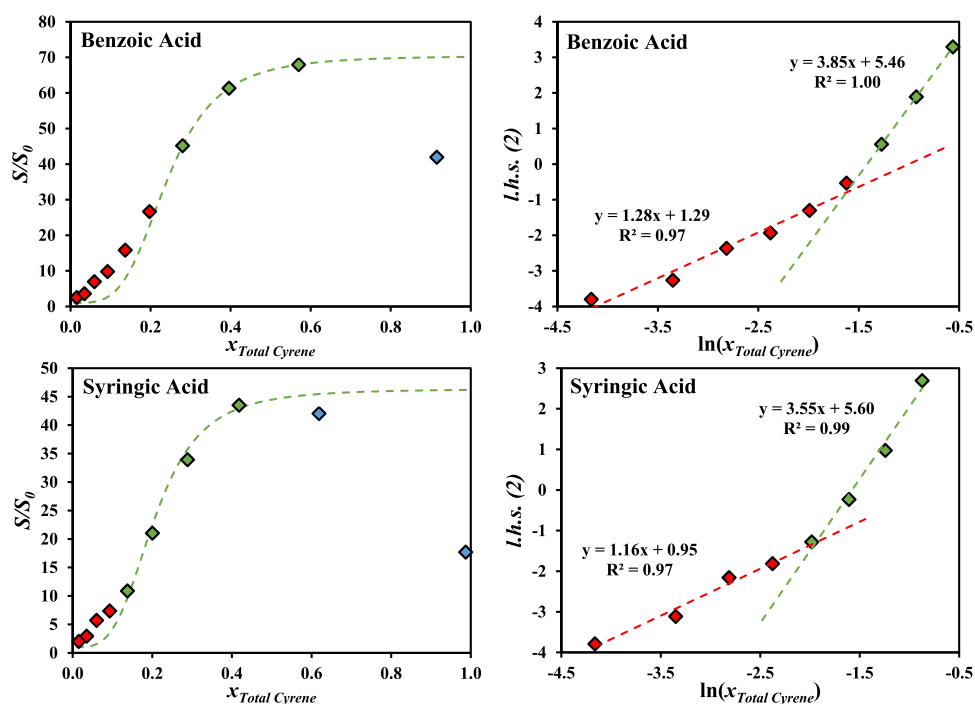


**Figure 3.** Left: solubility increase ( $S/S_0$ ) of the hydrophobic solute (red diamond, green diamond, blue diamond) along with the fitted curves of the cooperative hydrotropy model using the red data points (red dashed line) and the green data points (green dashed line). Right: a linearized form of eq 2, where the  $y$ -axis is the left-hand side of eq 2.

corresponding to the solubility maximum. These results are reported in Figure 3 (left) along with the left-hand side of eq 2 as a function of  $\ln(x_{\text{total Cyrene}})$  (Figure 3, right), which is an intuitive way of understanding the change in the dissolution regime. As is explained below, this is not a limitation of the model; instead, the necessity for two different fittings stems from the transition between the diol form as the main hydrotrope to the ketone form as the main hydrotrope.

From the application of the cooperative hydrotropy model reported in Figure 3, it is evident that the solubility curves of hydrophobic solutes in water–Cyrene mixtures can be divided into three regions, depending on the concentration of Cyrene. At a low concentration of Cyrene ( $x_{\text{total Cyrene}}$  from 0 to about 0.2), the  $m$  parameter of the model takes a value of around 1. Then, there is a sharp transition (Figure 3, right), and at a medium concentration of Cyrene ( $x_{\text{total Cyrene}}$  from about 0.2 until solubility maximum is attained), the  $m$  parameter takes a value of around 4. Finally, the occurrence of the maximum and consequent solubility decrease indicates that, above a certain concentration of Cyrene, water is no longer the principal solvent of the system and hydrotropy is replaced by another mechanism of solvation. Note that, due to its underlying assumptions, the cooperative hydrotropy model can only describe increases in solubility but cannot describe maxima or solubility decrease.

The results of Figure 3 are remarkable, especially considering that the cooperative hydrotropy model is applied using only one adjustable parameter ( $\delta_{\text{max}}$ ), and are a strong indicator that the mechanism of solvation in the water–Cyrene system, in most of its concentration range, is, in fact, hydrotropy (herein defined as water-mediated aggregation of hydrotrope molecules around the solute<sup>25</sup>). Bearing in mind that (i) hydrotropy is driven by the apolarity of both the solute and the hydrotrope<sup>25</sup> and (ii) the ketone form of Cyrene is much more hydrophobic than its diol form, the parameter

transition reported in Figure 3, occurring at around  $x_{\text{total Cyrene}} = 0.2$ , can be interpreted as hydrotropy occurring mainly due to aggregation of the diol form around the solute for low concentrations of Cyrene and aggregation of the ketone form around the solute at high concentrations of Cyrene. Since the ketone form is more hydrophobic than the diol form, the driving force of hydrotropy is larger with the former than the latter, leading to a much greater  $m$  value or, in other words, leading to more hydrotrope molecules aggregating around the solute and, thus, better solubility enhancement.

Figure 2 reveals that a total Cyrene mole fraction of around 0.3 maximizes the amount of geminal diol form present in the water–Cyrene system. Interestingly, Figure 3 reveals that the maximum in solubility of the hydrophobic solutes studied occurs at a total Cyrene mole fraction much greater than 0.3 when the concentration of the diol is less than 20%. If the geminal diol was in fact the component responsible for the hydrotropic ability of the system, as suggested by De bruyn et al.,<sup>14</sup> the maximum in solubility should appear at much lower concentrations of Cyrene. This, coupled with the results of Figure 3 and the discussion of the last paragraph, strongly suggests that the principal component driving solubilization is the ketone form of Cyrene, with the geminal diol playing a secondary role, in line with the foundations of the cooperative theory of hydrotropy. It is not being claimed, though, that the diol form of Cyrene does not act as a hydrotrope. As revealed in Figure 3, for low concentrations of Cyrene where its ketone form is virtually absent, the diol form indeed acts as a hydrotrope, but with much lower efficiency than the ketone form. Furthermore, it is also not being claimed that only the diol form of Cyrene acts as a hydrotrope at low concentration and that only the ketone form of Cyrene acts as a hydrotrope at large concentration. The aggregation of hydrotropes around the solute is statistical; these are short-lived clusters without a definite structure, unlike, for instance, micelles. As such, it is

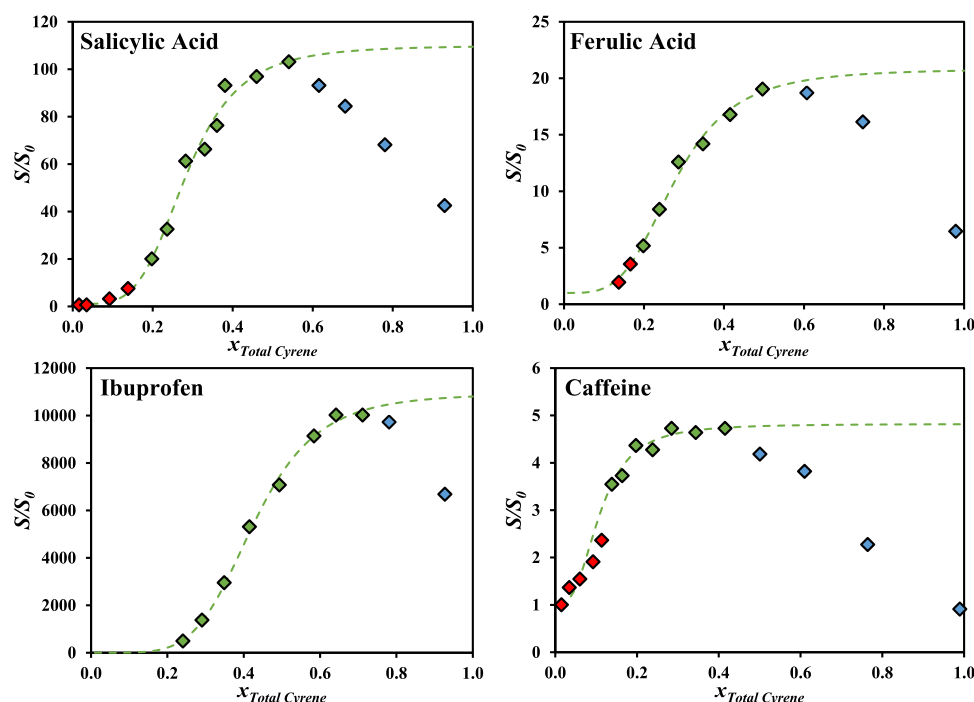


**Figure 4.** Solubility increase ( $S/S_0$ ) of the hydrophobic solute as a function of total Cyrene mole fraction (red diamond, green diamond, blue diamond) along with the fitting curves of the cooperative model using only the green data points (green dashed line). Data by De Bruyn et al.<sup>14</sup>

plausible that the ketone and diol forms of Cyrene both aggregate at the same time around the solute. However, what the cooperative hydrotrophy model shows is that the driving force for aggregation (quantified by  $m^{25}$ ) between the diol form and the solute is much lower than that between the ketone form and the solute. Thus, aggregation of the ketone form around the solute becomes predominant as the concentration of Cyrene increases. This is why  $x_{\text{total Cyrene}}$  is used in the fitting of the cooperative hydrotrophy model, instead of the mole fractions of the individual Cyrene forms.

Having established that the ketone form of Cyrene is the principal hydrotrope in the water–Cyrene system, the solubility curves of salicylic acid, ferulic acid, ibuprofen, and caffeine in the water–Cyrene system are now studied. These are depicted in Figure 4, along with the cooperative hydrotrophy model fitted to the green data points, as explained above. Note that data on the solubility of mandelic acid is also available,<sup>14</sup> but, unlike the other solutes mentioned, mandelic acid significantly disrupts the ketone–diol equilibrium of Cyrene,<sup>28</sup> hampering its analysis, most likely due to its much higher solubility in pure water. It is, thus, left out of this analysis.

In a similar way to Figure 3, Figure 4 shows that the cooperative hydrotrophy model is able to describe the solubility enhancement of hydrophobic solutes due to the presence of Cyrene, reinforcing that hydrotrophy is indeed the mechanism of solvation in most of its concentration range. The parameters of the cooperative hydrotrophy model ( $m$ ,  $b$ , and  $\delta_{\text{max}}$ ) for the solubility curves depicted in Figures 3 and 4 are reported in Table 2.

The parameter  $m$  of the cooperative hydrotrophy model is interpreted as the effective number of hydrotrope molecules aggregated around the solute. It has been shown that, for a given solute and a series of homologous hydrotropes,  $m$  increases with the apolar volume of the hydrotrope until the apolar volumes of the solute and the hydrotrope match, decreasing thereafter.<sup>25</sup> That is, the larger the apolar volume of

**Table 2.** Parameters of the Cooperative Model Fitted to the Cyrene-Based Hydrotropic Systems Studied in This Work Along With the Logarithm of the Partition Coefficient between Octanol and Water of the Solutes

substance	max	$m$	$b$	$\log(K_{O,W})^{29}$
benzoic acid	70	3.85	5.46	1.87
syringic acid	46	3.55	5.60	1.04
salicylic acid	110	4.28	5.39	2.26
ferulic acid	21	3.75	4.80	1.51
ibuprofen	10 935	5.17	4.40	3.97
caffeine	5	2.87	6.37	0.07

the hydrotrope, the weaker the interaction with water and the greater the driving force for aggregation with the solute, as first proposed by Kunz and co-authors.<sup>26</sup> However, when the hydrotrope has a larger apolar volume than the solute, the driving force for hydrotrope–hydrotrope aggregation is greater than that of solute–hydrotrope aggregation, leading to a decrease in  $m$ .<sup>25</sup>

In contrast with the example above, several solutes are studied for the same hydrotrope in this work. It is, thus, expected that  $m$  increases with the apolarity of the solute. To test this hypothesis, the hydrophobicity of the solutes studied above (benzoic acid, syringic acid, salicylic acid, ferulic acid, ibuprofen, and caffeine) was quantified using the logarithm of their octanol/water partition coefficients ( $K_{O,W}$ ). This parameter, listed in Table 2 for each solute, is a measure of the preference of the solute to be solvated by an apolar medium instead of water or, more correctly, is a measure of the preference of water to not solvate the solute. Within the framework of cooperative hydrotrophy, it makes sense that the number of hydrotropes aggregated around the solute through their apolar moieties (quantified by  $m$ ) is proportional to the preference of the solute to be surrounded by an apolar medium

(quantified by  $K_{O,W}$ ). Figure 5 depicts the correlation obtained between  $m$  and  $\log(K_{O,W})$ .

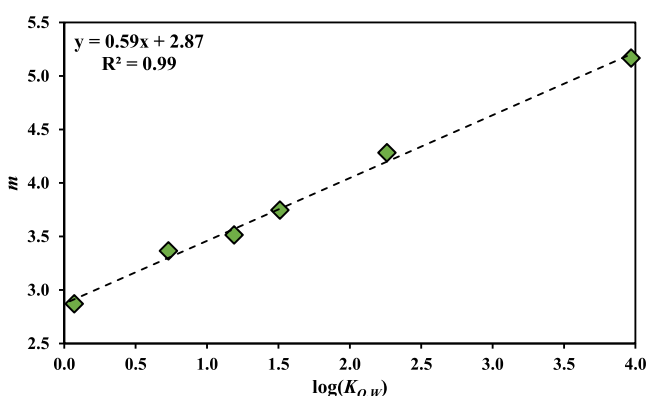


**Figure 5.** Parameter  $m$  of the cooperative hydrotrophy model for the hydrophobic solutes studied in this work as a function of the logarithm of the partition coefficient between octanol and water of the solute. The dashed line is the fitted line using the least-squares method (coefficient of determination is 0.99).

Figure 5 reveals an excellent correlation between  $m$  and  $\log(K_{O,W})$ . Again, this is interpreted as the number of hydrotrope molecules around the solute being dependent on the preference of the solute to be surrounded by apolar moieties instead of water molecules. These results support the idea of apolarity as the driving force of hydrotrophy<sup>25</sup> and complement those previously reported for glycerol ethers. Note that the dependence of  $m$  on the apolar volume of the solute is anticipated. In other words, the larger the solute, the greater the number of hydrotrope molecules needed to cover its apolar area. However, the apolar size of the solute is encoded in  $\log(K_{O,W})$  since the apolar size plays a role in the partition from water to an apolar medium.

The success of  $\log(K_{O,W})$  in describing  $m$  suggests that there may be similar correlations for  $\delta_{\max}$  and  $b$ . Finding such correlations not only helps to understand the mechanism of hydrotrophy but would also add an important predictive component to the cooperative hydrotrophy model, allowing the prediction of the solubility of hydrophobic substances in water–Cyrene mixtures. In fact,  $\log(\delta_{\max})$ , as depicted in Figure 6, also correlates remarkably well with  $\log(K_{O,W})$ .

By definition,  $\delta_{\max}$  can be interpreted as the partition coefficient of the solute between water and the hydrotropic system, measured at solute saturation instead of solute dilution. As such, the correlation depicted in Figure 6 bears a resemblance to the work of Collander,<sup>30</sup> where it was shown that the partition coefficient of a solute between a solvent and water ( $K_1$ ) could be correlated to the partition coefficient of the same solute but between a different solvent and water ( $K_2$ ) according to the following expression

$$\log(K_1) = a \cdot \log(K_2) + b \quad (3)$$

where  $a$  and  $b$  are the slope and intercept of the line obtained by plotting  $\log(K_1)$  against  $\log(K_2)$ . Even though the physical meaning of these parameters is not clear,<sup>31</sup> eq 3 is known to yield a better correlation when the organic solvents are similar. In this sense, the correlation depicted in Figure 6 could be improved by defining a partition coefficient between Cyrene and water

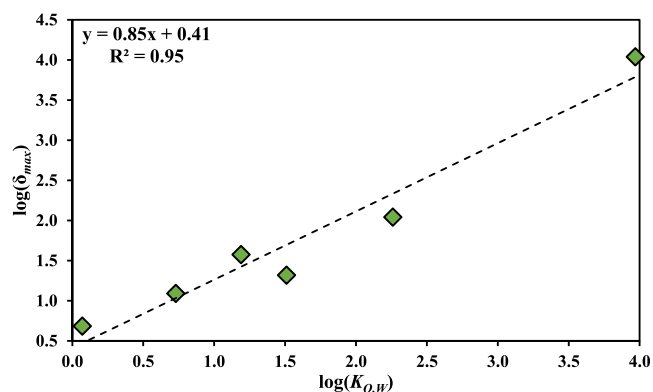


**Figure 6.** Logarithm of parameter  $\delta_{\max}$  of the cooperative hydrotrophy model for the hydrophobic solutes studied in this work as a function of the logarithm of the partition coefficient between octanol and water of the solute. The dashed line is the fitted line using the least-squares method (coefficient of determination is 0.95).

$$P_{C,W}^* = \frac{S_{\text{Cyrene}}}{S_{\text{water}}} \quad (4)$$

where  $S_{\text{Cyrene}}$  and  $S_{\text{water}}$  is the molar solubility of the solute in Cyrene and water, respectively, and \* emphasizes that this partition coefficient is calculated from the solute solubility as opposed to solute dilution. Figure 7 depicts the correlation

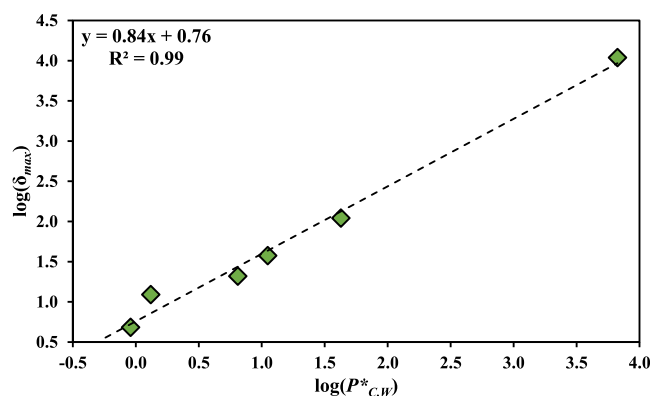


**Figure 7.** Logarithm of parameter  $\delta_{\max}$  of the cooperative hydrotrophy model for the hydrophobic solutes studied in this work as a function of the logarithm of the solubility ratio of the solute between pure Cyrene and pure water. The dashed line is the fitted line using the least-squares method (coefficient of determination is 0.99).

obtained between  $\log(\delta_{\max})$  and  $\log(P_{C,W}^*)$ . Even though it is clear that this correlation is better than that reported in Figure 6, it loses some of its predictive character since the solubility of the solute in pure water and pure Cyrene must be experimentally available, which is seldom the case, even when the hydrotrope is a liquid. It nevertheless reinforces and supports the correlation with  $\log(K_{O,W})$  presented above.

So far, both  $m$  and  $\delta_{\max}$  have been successfully correlated with the apolarity of the solute (quantified by  $\log(K_{O,W})$ ). Contrary to these parameters, although the parameter  $b$  of the cooperative hydrotrophy model may seem to pertain to a property of the hydrotrope (fugacity of inserting  $m$  hydrotrope molecules in the volume corresponding to the vicinity of the solute) and not of the solute, it depends on the number of hydrotropes to be inserted ( $m$ ) around the solute, which, in turn, depends on the hydrophobicity of the solute, as shown in

Figure 5. As such, a decent correlation can be obtained between  $b$  and  $\log(K_{O,W})$ , as depicted in Figure 8.

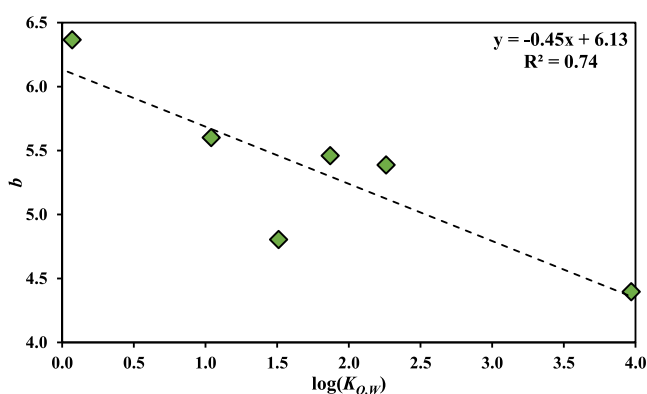


**Figure 8.** Parameter  $b$  of the cooperative hydrotrophy model for the hydrophobic solutes studied in this work as a function of the logarithm of the partition coefficient between octanol and water of the solute. The dashed line is the fitted line using the least-squares method (coefficient of determination is 0.74).

The correlations here reported for the parameters of the cooperative hydrotrophy model ( $m$ ,  $b$ , and  $\delta_{\max}$ ) support the notion that hydrotrophy depends on the apolarity of both the solute and the hydrotrope. This is in line with previous studies<sup>18,25</sup> and contradicts the notion that only the hydrophobic volume of the hydrotrope is a major factor influencing hydrotrophy.<sup>26</sup>

**3.3. Solubility Prediction.** So far, we have shown the usefulness of the cooperative hydrotrophy model to describe the solubility of hydrophobic solutes in water–Cyrene mixtures. It must be highlighted that the correlations herein obtained are not purely empirical, since they possess physical meaning and can be interpreted in terms of the cooperative mechanism of hydrotrophy and the foundations of its statistical thermodynamics-based model.

The correlations proposed for parameters  $m$ ,  $b$ , and  $\delta_{\max}$  add a predictive character to the cooperative hydrotrophy model. This is explored in this section by predicting the solubility curves of phthalic acid, aspirin, gallic acid, and vanillin in water–Cyrene mixtures. The choice of gallic acid and vanillin is based on their bioactivity, such as their antioxidant properties, and the fact that they are present in a wide variety of natural sources.<sup>32–36</sup> Moreover, they can be regarded as model molecules of lignin, making their study an important step in understanding the solubilization of this important natural polymer.<sup>19,37,38</sup>

The values obtained for the parameters of the cooperative hydrotrophy model, using the correlations depicted in Figures 5, 6, and 8, are reported in Table 3 for the new solutes. The predicted solubility curves of phthalic acid, aspirin, gallic acid, and vanillin are depicted in Figure 9.

Figure 9 reveals that the framework developed in this work can be used to successfully predict the solubility of hydrophobic solutes in water–Cyrene mixtures. Note that the predictions for gallic acid and vanillin are not as accurate as those for phthalic acid and aspirin. This is probably due to the difference in temperature: the solubility data explored throughout this work was measured at 20 °C, while the data reported for gallic acid and vanillin was measured at 30 °C. The data for these two solutes was herein experimentally

**Table 3.** Logarithm of the Partition Coefficient between Octanol and Water, Along With the Predicted  $m$  and  $\delta_{\max}$  Parameters of the Cooperative Hydrotrophy Model for the Solutes Whose Solubility Is Predicted in This Work

solute	$\log(K_{O,W})$ <sup>29</sup>	$m$	$\delta_{\max}$	$b$
phthalic acid	0.73	3.30	11	5.80
aspirin	1.19	3.57	26	5.59
gallic acid	0.7	3.28	10	5.82
vanillin	1.37	3.68	38	5.51

measured at 30 °C for two different reasons: first, to check the influence of temperature on the accuracy of the predictive methodology herein developed and, thus, the extent of its applicability and, second, to report data for gallic acid and vanillin at 30 °C, facilitating future comparisons of the efficiency of Cyrene as a hydrotrope against previously reported hydrotropes in the literature, whose solubility enhancement for gallic acid and vanillin was reported at 30 °C.<sup>18,20</sup>

With respect to the influence of temperature on the prediction of solubility, Figure 9 shows that the maximum solubility enhancement prediction is accurate and not strongly influenced by temperature. This is reasonable since the maximum solubility enhancement is a ratio between solute solubility in the mixture and in water, which may be quantitatively affected by temperature in the same way. However, the onset of hydrotrophy (represented by parameters  $m$  and  $b$ ) seems to occur at lower concentrations of Cyrene when the temperature is increased (see Figure S6 of the Supporting Information for a comparison between the solubility of syringic acid in water–Cyrene mixtures at 20 and 30 °C), which may be explored to improve the efficiency of Cyrene as a hydrotrope.

## 4. CONCLUSIONS

The development of new applications for the water–Cyrene system, namely, those related to its solubilization ability, has been limited by a lack of fundamental understanding of this system. In this work, the quantitative framework to consistently study the solubility of hydrophobic solutes in this solvent was introduced. Then, the cooperative hydrotrophy model was applied to data previously reported in the literature along with novel data measured in this work, which led to the conclusion that the ketone form of Cyrene, and not its diol form as claimed in the literature, is the major component responsible for the solubility increase of hydrophobic solutes in water–Cyrene mixtures.

The parameters obtained by fitting the cooperative hydrotrophy model to the experimental solubility data were discussed in terms of their physical meaning. It was found that  $m$ , the effective number of hydrotrope molecules aggregated around a solute molecule, correlates remarkably well with the apolarity of the solutes, which was quantified using the logarithm of their octanol–water partition coefficients. Furthermore, the parameter  $\delta_{\max}$  which corresponds to the maximum attainable solubility increase of the solute, should the mechanism of hydrotrophy prevail in the entire concentration range of the water–Cyrene system, was also shown to have an excellent correlation with the apolarity of the solute. Finally, parameter  $b$ , which represents the fugacity of inserting  $m$  hydrotrope molecules in the bulk solution with the volume corresponding to the vicinity volume of the solute, was shown to also

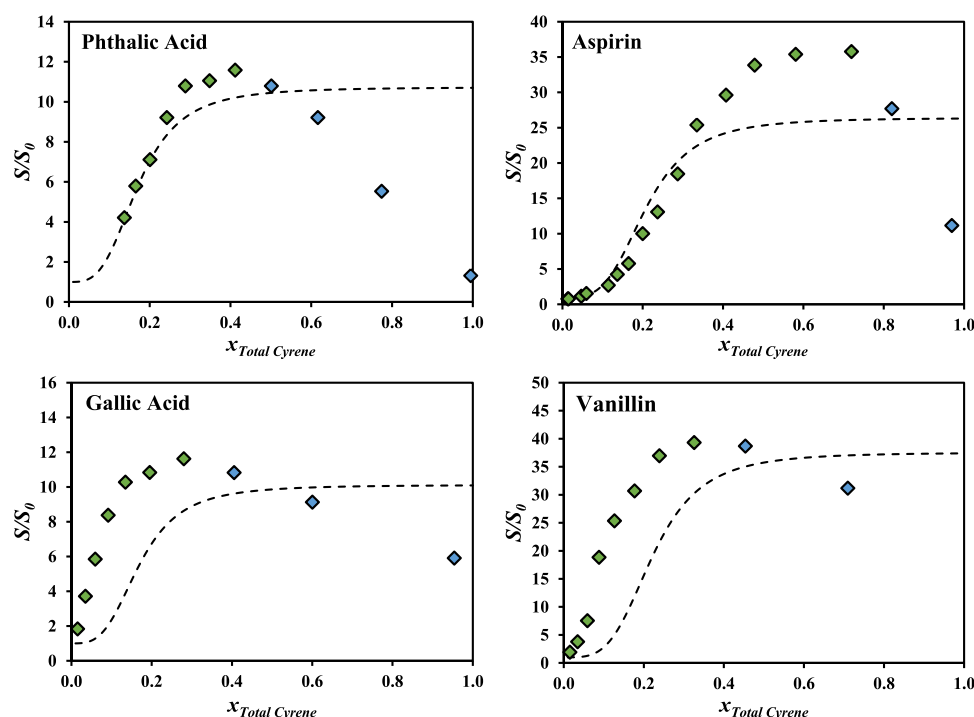


**Figure 9.** Experimental solubility increase ( $S/S_0$ ) of hydrophobic solutes as a function of total Cyrene mole fraction (green diamond, blue diamond) along with the predicted solubility increase using the cooperative hydrotropy model and the correlations constructed throughout this work (dashed lines). Data from De bruyn et al.<sup>14</sup> (phthalic acid and aspirin, measured at 20 °C) and this work (gallic acid and vanillin, measured at 30 °C).

correlate with the apolarity of the solute, stemming from its dependence on the number of aggregated hydrotropic molecules around the solute ( $m$ ).

The correlations obtained for the parameters of the cooperative hydrotropy model allowed for the prediction of the solubility of phthalic acid, aspirin, gallic acid, and vanillin in water–Cyrene mixtures. As such, it is herein shown, for the first time, that a consistent study of solubility for a single hydrotropic, varying only the solutes, allows for the parametrization of the cooperative hydrotropy model, which can then be used to predict the solubility of any hydrophobic solute in water mixtures of that hydrotropic. In other words, the procedure reported in this work can be perceived as a parametrization procedure for the cooperative hydrotropy model.

The results herein reported pave the way for future work on solubility studies with water–Cyrene mixtures. For instance, it is now known that hydrotropy does not occur at high Cyrene concentrations, but the mechanism present in that concentration range is unknown. Furthermore, since it was shown that the ketone form of Cyrene is a better hydrotropic than the diol form, finding a way to manipulate the extent of the equilibrium of Cyrene in water would permit the maximization of the concentration of the ketone form, which, in turn, would maximize the solubility potential of water–Cyrene mixtures. This cannot, however, be achieved by acidifying the medium, as suggested by the UV results reported in this work.

## ■ ASSOCIATED CONTENT

### SI Supporting Information

The Supporting Information is available free of charge at <https://pubs.acs.org/doi/10.1021/acs.iecr.0c02346>.

Additional acidity analysis, calculation details, and solubility data; pH of water–Cyrene mixtures (Figure S1); UV spectra of water–Cyrene mixtures (Figure S2); impact of pH on the composition of water–Cyrene mixtures (Figure S3); composition of water–Cyrene mixtures (Figure S4); density of water–Cyrene mixtures (Figure S5); solubility of syringic acid in water–Cyrene mixtures (Figure S6); and solubility of the studied compounds in water–Cyrene mixtures (Tables S1–S3) (PDF)

## ■ AUTHOR INFORMATION

### Corresponding Author

João A. P. Coutinho – CICECO—Aveiro Institute of Materials, Department of Chemistry, University of Aveiro, 3810-193 Aveiro, Portugal; [orcid.org/0000-0002-3841-743X](https://orcid.org/0000-0002-3841-743X); Email: [jcoutinho@ua.pt](mailto:jcoutinho@ua.pt)

### Authors

Dinis O. Abranches – CICECO—Aveiro Institute of Materials, Department of Chemistry, University of Aveiro, 3810-193 Aveiro, Portugal; [orcid.org/0000-0003-0097-2072](https://orcid.org/0000-0003-0097-2072)

Jordana Benfica – CICECO—Aveiro Institute of Materials, Department of Chemistry, University of Aveiro, 3810-193 Aveiro, Portugal; [orcid.org/0000-0002-6437-1383](https://orcid.org/0000-0002-6437-1383)

Seishi Shimizu – York Structural Biology Laboratory, Department of Chemistry, University of York, York YO10 SDD, United Kingdom; [orcid.org/0000-0002-7853-1683](https://orcid.org/0000-0002-7853-1683)

Complete contact information is available at:

<https://pubs.acs.org/doi/10.1021/acs.iecr.0c02346>

### Notes

The authors declare no competing financial interest.

## ACKNOWLEDGMENTS

This work was developed within the scope of the project CICECO-Aveiro Institute of Materials, UIDB/50011/2020 and UIDP/50011/2020 financed by national funds through the FCT/MEC, and when appropriate, cofinanced by FEDER under the PT2020 Partnership Agreement. Support was provided by the AllNat project - POCI-01-0145-FEDER-030463 (PTDC / EQU-EPQ / 30463/2017), financed by ERDF funds through COMPETE2020 - Competitiveness and Internationalization Operational Program (POCI). FCT is also acknowledged for the financial support through the project SAICTPAC/0040/2015.

## REFERENCES

- (1) Sherwood, J.; De bruyn, M.; Constantinou, A.; Moity, L.; McElroy, C. R.; Farmer, T. J.; Duncan, T.; Raverty, W.; Hunt, A. J.; Clark, J. H. Dihydrolevoglucosenone (Cyrene) as a Bio-Based Alternative for Dipolar Aprotic Solvents. *Chem. Commun.* **2014**, *50*, 9650–9652.
- (2) Kudo, S.; Goto, N.; Sperry, J.; Norinaga, K.; Hayashi, J. Production of Levoglucosenone and Dihydrolevoglucosenone by Catalytic Reforming of Volatiles from Cellulose Pyrolysis Using Supported Ionic Liquid Phase. *ACS Sustainable Chem. Eng.* **2017**, *5*, 1132–1140.
- (3) Cao, F.; Schwartz, T. J.; McClelland, D. J.; Krishna, S. H.; Dumesic, J. A.; Huber, G. W. Dehydration of Cellulose to Levoglucosenone Using Polar Aprotic Solvents. *Energy Environ. Sci.* **2015**, *8*, 1808–1815.
- (4) Bouxin, F. P.; Clark, J. H.; Fan, J.; Budarin, V. Combining Steam Distillation with Microwave-Assisted Pyrolysis to Maximise Direct Production of Levoglucosenone from Agricultural Wastes. *Green Chem.* **2019**, *21*, 1282–1291.
- (5) Mistry, L.; Mapesa, K.; Bousfield, T. W.; Camp, J. E. Synthesis of Ureas in the Bio-Alternative Solvent Cyrene. *Green Chem.* **2017**, *19*, 2123–2128.
- (6) Mention, M. M.; Flourat, A. L.; Peyrot, C.; Allais, F. Biomimetic Regioselective and High-Yielding Cu(I)-Catalyzed Dimerization of Sinapate Esters in Green Solvent Cyrene: Towards Sustainable Antioxidant and Anti-UV Ingredients. *Green Chem.* **2020**, *22*, 2077–2085.
- (7) Guajardo, N.; de María, P. D. Assessing Biocatalysis Using Dihydrolevoglucosenone (Cyrene) as Versatile Bio-Based (Co)-solvent. *Mol. Catal.* **2020**, *485*, No. 110813.
- (8) Ferrazzano, L.; Corbisiero, D.; Martelli, G.; Tolomelli, A.; Viola, A.; Ricci, A.; Cabri, W. Green Solvent Mixtures for Solid-Phase Peptide Synthesis: A Dimethylformamide-Free Highly Efficient Synthesis of Pharmaceutical-Grade Peptides. *ACS Sustainable Chem. Eng.* **2019**, *7*, 12867–12877.
- (9) Wilson, K. L.; Murray, J.; Jamieson, C.; Watson, A. J. B. Cyrene as a Bio-Based Solvent for HATU Mediated Amide Coupling. *Org. Biomol. Chem.* **2018**, *16*, 2851–2854.
- (10) Bousfield, T. W.; Pearce, K. P. R.; Nyamini, S. B.; Angelis-Dimakis, A.; Camp, J. E. Synthesis of Amides from Acid Chlorides and Amines in the Bio-Based Solvent Cyrene. *Green Chem.* **2019**, *21*, 3675–3681.
- (11) Zhang, J.; White, G. B.; Ryan, M. D.; Hunt, A. J.; Katz, M. J. Dihydrolevoglucosenone (Cyrene) As a Green Alternative to N,N-Dimethylformamide (DMF) in MOF Synthesis. *ACS Sustainable Chem. Eng.* **2016**, *4*, 7186–7192.
- (12) Ray, P.; Hughes, T.; Smith, C.; Hibbert, M.; Saito, K.; Simon, G. P. Development of Bio-Acrylic Polymers from Cyrene: Transforming a Green Solvent to a Green Polymer. *Polym. Chem.* **2019**, *10*, 3334–3341.
- (13) Salavagione, H. J.; Sherwood, J.; De bruyn, M.; Budarin, V. L.; Ellis, G. J.; Clark, J. H.; Shuttleworth, P. S. Identification of High Performance Solvents for the Sustainable Processing of Graphene. *Green Chem.* **2017**, *19*, 2550–2560.
- (14) De bruyn, M.; Budarin, V. L.; Misefari, A.; Shimizu, S.; Fish, H.; Cockett, M.; Hunt, A. J.; Hofstetter, H.; Weckhuysen, B. M.; Clark, J. H.; et al. Geminal Diol of Dihydrolevoglucosenone as a Switchable Hydrotrope: A Continuum of Green Nanostructured Solvents. *ACS Sustainable Chem. Eng.* **2019**, *7*, 7878–7883.
- (15) Hodgdon, T. K.; Kaler, E. W. Hydrotropic Solutions. *Curr. Opin. Colloid Interface Sci.* **2007**, *12*, 121–128.
- (16) Dhapte, V.; Mehta, P. Advances in Hydrotropic Solutions: An Updated Review. *St. Petersburg Polytech. Univ. J.: Phys. Math.* **2015**, *1*, 424–435.
- (17) Anastas, P.; Eghbali, N. Green Chemistry: Principles and Practice. *Chem. Soc. Rev.* **2010**, *39*, 301–312.
- (18) Soares, B. P.; Abranches, D. O.; Sintra, T. E.; Leal-Duaso, A.; García, J. I.; Pires, E.; Shimizu, S.; Pinho, S. P.; Coutinho, J. A. P. Glycerol Ethers as Hydrotropes and Their Use to Enhance the Solubility of Phenolic Acids in Water. *ACS Sustainable Chem. Eng.* **2020**, *8*, 5742–5749.
- (19) Soares, B.; Silvestre, A. J. D.; Rodrigues Pinto, P. C.; Freire, C. S. R.; Coutinho, J. A. P. Hydrotropy and Cosolvency in Lignin Solubilization with Deep Eutectic Solvents. *ACS Sustainable Chem. Eng.* **2019**, *7*, 12485–12493.
- (20) Cláudio, A. F. M.; Neves, M. C.; Shimizu, K.; Canongia Lopes, J. N.; Freire, M. G.; Coutinho, J. A. P. The Magic of Aqueous Solutions of Ionic Liquids: Ionic Liquids as a Powerful Class of Catanionic Hydrotropes. *Green Chem.* **2015**, *17*, 3948–3963.
- (21) De bruyn, M.; Sener, C.; Petrolini, D. D.; McClelland, D. J.; He, J.; Ball, M. R.; Liu, Y.; Martins, L.; Dumesic, J. A.; Huber, G. W.; et al. Catalytic Hydrogenation of Dihydrolevoglucosenone to Levoglucosan with a Hydrotalcite/mixed Oxide Copper Catalyst. *Green Chem.* **2019**, *21*, 5000–5007.
- (22) Shimizu, S.; Matubayasi, N. The Origin of Cooperative Solubilisation by Hydrotropes. *Phys. Chem. Chem. Phys.* **2016**, *18*, 25621–25628.
- (23) Shimizu, S.; Matubayasi, N. Hydrotropy: Monomer–Micelle Equilibrium and Minimum Hydrotrope Concentration. *J. Phys. Chem. B* **2014**, *118*, 10515–10524.
- (24) Nicol, T. W. J.; Isobe, N.; Clark, J. H.; Shimizu, S. Statistical Thermodynamics Unveils the Dissolution Mechanism of Cellobiose. *Phys. Chem. Chem. Phys.* **2017**, *19*, 23106–23112.
- (25) Abranches, D. O.; Benfica, J.; Soares, B. P.; Leal-Duaso, A.; Sintra, T. E.; Pires, E.; Pinho, S. P.; Shimizu, S.; Coutinho, J. A. P. Unveiling the Mechanism of Hydrotropy: Evidence for Water-Mediated Aggregation of Hydrotropes around the Solute. *Chem. Commun.* **2020**, *56*, 7143–7146.
- (26) Bauduin, P.; Renoncourt, A.; Kopf, A.; Touraud, D.; Kunz, W. Unified Concept of Solubilization in Water by Hydrotropes and Cosolvents. *Langmuir* **2005**, *21*, 6769–6775.
- (27) Buschmann, H.-J.; Fuldner, H.-H.; Knoche, W. The Reversible Hydration of Carbonyl Compounds in Aqueous Solution. Part I, The Keto/Gem-Diol Equilibrium. *Ber. Bunsengesell. Phys. Chem.* **1980**, *84*, 41–44.
- (28) Misefari, A. *Investigation of the Spectroscopic, Chemical and Physical Properties of Cyrene and Its Hydrate*; University of York, 2017.
- (29) Kim, S.; Chen, J.; Cheng, T.; Gindulyte, A.; He, J.; He, S.; Li, Q.; Shoemaker, B. A.; Thiessen, P. A.; Yu, B.; et al. PubChem 2019 Update: Improved Access to Chemical Data. *Nucleic Acids Res.* **2019**, *47*, D1102–D1109.
- (30) Collander, R. The Partition of Organic Compounds Between Higher Alcohols and Water. *Acta Chem. Scand.* **1951**, *5*, 774–780.
- (31) Beezer, A. E.; Gooch, C. A.; Hunter, W. H.; Volpe, P. L. O. A Thermodynamic Analysis of the Collander Equation and Establishment of a Reference Solvent for Use in Drug Partitioning Studies. *J. Pharm. Pharmacol.* **1987**, *39*, 774–779.
- (32) Teixeira, J.; Silva, T.; Benfeito, S.; Gaspar, A.; Garrido, E. M.; Garrido, J.; Borges, F. Exploring Nature Profits: Development of Novel and Potent Lipophilic Antioxidants Based on Galloyl–cinnamic Hybrids. *Eur. J. Med. Chem.* **2013**, *62*, 289–296.
- (33) Srinivasulu, C.; Ramgopal, M.; Ramanjaneyulu, G.; Anuradha, C. M.; Suresh Kumar, C. Syringic Acid (SA) – A Review of Its

Occurrence, Biosynthesis, Pharmacological and Industrial Importance. *Biomed. Pharmacother.* **2018**, *108*, 547–557.

(34) Burri, J.; Graf, M.; Lambelet, P.; Löliger, J. Vanillin: More than a Flavouring Agent—a Potent Antioxidant. *J. Sci. Food Agric.* **1989**, *48*, 49–56.

(35) Badhani, B.; Sharma, N.; Kakkar, R. Gallic Acid: A Versatile Antioxidant with Promising Therapeutic and Industrial Applications. *RSC Adv.* **2015**, *5*, 27540–27557.

(36) Govardhan Singh, R. S.; Negi, P. S.; Radha, C. Phenolic Composition, Antioxidant and Antimicrobial Activities of Free and Bound Phenolic Extracts of Moringa Oleifera Seed Flour. *J. Funct. Foods* **2013**, *5*, 1883–1891.

(37) Santos, J. H. P. M.; Martins, M.; Silvestre, A. J. D.; Coutinho, J. A. P.; Ventura, S. P. M. Fractionation of Phenolic Compounds from Lignin Depolymerisation Using Polymeric Aqueous Biphasic Systems with Ionic Surfactants as Electrolytes. *Green Chem.* **2016**, *18*, 5569–5579.

(38) Soares, B.; Tavares, D. J. P.; Amaral, J. L.; Silvestre, A. J. D.; Freire, C. S. R.; Coutinho, J. A. P. Enhanced Solubility of Lignin Monomeric Model Compounds and Technical Lignins in Aqueous Solutions of Deep Eutectic Solvents. *ACS Sustainable Chem. Eng.* **2017**, *5*, 4056–4065.